Sgr A East as a possible high energy neutron factory in the Galactic Centre

Dario Grasso[1,2] †, Luca Maccione[2,3] ‡

February 2, 2008

[1] Scuola Normale Superiore, P.zza Dei Cavalieri, 7, I-56126 PISA
[2] I.N.F.N. Sezione di Pisa
[3] Dip. di Fisica "E. Fermi", Università di Pisa, Largo B. Pontecorvo, 3, PISA

† d.grasso@sns.it; ‡ luca.maccione@pi.infn.it

Abstract

Sgr A East is a supernova remnant located within few parsecs from the Galactic Centre (GC). There are good reasons to believe that this object is the source of the γ-ray excess detected by HESS in the direction of the GC meaning that Sgr A East is likely to be an efficient Cosmic Ray (CR) accelerator. Some observations suggest that strong magnetic fields may be present in that region which may allow the acceleration of composite nuclei in Sgr A East beyond the EeV. We show that, if this is case, EeV neutrons should be effectively produced by the photo-disintegration of Ultra High Energy nuclei onto the infrared photon background (with temperature ~ 40 K) in which Sgr A East is embedded. Neutrons with such an energy can reach the Earth before decaying and may be detectable under the form of a CR point-like excess in the direction of the GC. We determine the expected energy spectrum and the amplitude of this signal showing that it may be measurable by the AUGER observatory.

1 Introduction

One of the main puzzles in cosmic ray physics concerns the origin of cosmic rays (CRs) with energies between the knee ($E_{\rm knee} \sim 3 \times 10^{15}$ eV) and the ankle ($E_{\rm ankle} \sim 6 \times 10^{18}$ eV) of the CR spectrum. It is generally accepted that CRs with energy up to the knee are accelerated by the 'so-called' Fermi

first order mechanism (for a review see e.g. [1]) in the supersonic outflow of galactic SuperNova Remnants (SNRs). This wisdom is motivated not only by the well known coincidence between the galactic SN energy output and that of galactic CRs but also by the slope and the regularity of the CR energy spectrum over several energy decades. The observation of radio and γ-ray emissions from a number of SNRs provides further evidence of the validity of this scenario. It is more uncertain, however, what is the maximal energy $E_{\rm max}$ at which particles can be accelerated in this kind of sources. The continuity of the CR spectrum up to ankle suggests that the origin of CR above the knee is closely related to that below the knee meaning that $E_{\rm max}$ may be larger than the EeV.

One of the crucial quantities which enters to determine $E_{\rm max}$ is the magnetic field strength in the region where the SNR shell is expanding through. It is known that, if the mean value of the galactic magnetic field ($B_{\rm gal} \simeq 5\ \mu$G) is adopted, the theoretically estimated $E_{\rm max}$ cannot exceed the Lagage and Cesarsky bound $E_{\rm max}^{\rm LC} \sim Z \times 10^{16}$ eV [2]. Stronger magnetic fields may however be found in some dense regions of the Galaxy, like the Galactic Centre (GC) [3] or in dense molecular clouds [4]. It is also possible that non-linear effects, e.g. cosmic-ray streaming instabilities [5], give rise to an amplification of the magnetic field in the acceleration region allowing to reach CR energies exceeding the Lagage and Cesarsky bound. Even in this case, however, the largest CR energies are expected to be reached in SNRs placed in regions with the strongest magnetic field backgrounds.

It would be extremely interesting to find an observational evidence showing that CR acceleration up to Ultra High Energies (UHEs) ($E \gtrsim 10^{18}$ eV) takes place in some galactic SNR. Unfortunately, even EeV protons are significantly deflected in the galactic magnetic field so that the angular correlation between the arrival direction of these particles and the position of their sources should be spoiled. A possible way out may, however, be found if EeV secondary neutrons are efficiently produced by the scattering of the UHE primary nuclei with the matter and the radiation surrounding the SNR. Neutrons with such an energy can travel over galactic distances without undergoing significant decay and deflections. Although high energy neutrons and protons give rise to indistinguishable showers in the atmosphere, a galactic neutron source may be recognised by the extensive air shower experiments under the form of a localised excess of CRs with energy $\gtrsim 1$ EeV. Clearly, a complete identification of the source requires a matching between the position of the CR excess and that of a radio, X-ray and, possibly, γ-ray emitting SNR [6].

The SNRs which are the most promising sources of EeV neutrons are those residing in the densest regions of the Galaxy, where strong magnetic

fields as well as thick radiation and gas targets can presumably be found. Active SNRs in the proximity of the Galactic Center (GC) and/or in the nearby of dense molecular clouds are natural candidates to the role of EeV neutron factories.

In this respect, as it was recently suggested in [7], a particularly interesting system is Sgr A East. Sgr A East is a SNR located within few parsecs from the dynamical centre of the Galaxy. Detailed radio and X-ray observations [8, 9] allowed to conclude that this object is a mixed-morphology (radio shell + X-ray emitting core) remnant of a single type II SN explosion which took place between 10^4 and 10^5 years ago (the light propagation time is subtracted). This SNR is embedded within a dense ionised gas halo and in a background of Infrared (IR) radiation due to dust emission at the temperature $T \sim 40$ K [10, 11]. Furthermore, the expanding Sgr A East radio shell is interacting with a dense molecular cloud. Strong magnetic fields, as large as few milliGauss, have been observed in that region [3].

A γ-ray emission has been also recently observed by the HESS Cerenkov telescope in the direction of the GC [12]. Although the limited angular resolution reachable with this kind of observations did not allow a firm identification of the source of this emission, several arguments points to Sgr A East as the most plausible source. The most convincing among these arguments is based on the energetic of the emission observed by HESS. In Sec. 3 we show, in fact, that the γ-ray flux measured by HESS practically coincides with that expected from the decay of neutral pions produced in the hadronic collisions of UHE protons which are shock accelerated by a SNR with the same characteristics of Sgr A East. On the basis of this argument, as well as other arguments listed in Sec.3, we assume that Sgr A East accelerates nuclei with a power law spectrum with index equal to that of the γ-ray excess observed by HESS.

In Sec.4 we argue that the spectrum of CRs accelerated in Sgr A East may extend beyond the EeV.

EeV neutrons may be produced as secondary particles of UHE nuclei in Sgr A East by two main processes: the Photo-Disintegration (PD) of composite nuclei onto the 40 K IR photon background present in that region and the *pp* inelastic scattering of UHE protons onto the dense hydrogen gas. In this paper (see Sec.s 5 and 6) we estimate the expected neutron flux reaching the Earth produced by both processes. We show that PD should provide the dominant, if not the unique, contribution. This contribution was not computed in a previous work on the subject [7].

In Sec.7 we estimate the event rate expected at the Pierre AUGER Observatory [13] due to neutrons from Sgr A East.

The possibility that EeV neutrons could be produced by a SNR in the

GC giving rise to a localised CR excesses around the EeV has been already suggested in several papers (see e.g. [14, 15, 16]). In particular, Crocker *et al.* [7] first proposed Sgr A East as a possible high energy γ-ray and EeV neutron source, although the contribution of nuclei PD to the neutron flux was not determined in their paper. All these works, however, tried to interpret the EeV CR anisotropy claimed by the AGASA [14] and SUGAR [17] experiments. This is not what we do in this paper. Actually, in Sec.8 we argue that both AGASA and SUGAR anisotropies can hardly be ascribed to a neutron emission from the Galactic centre. In particular we show that the EeV neutron flux estimated in [7] is likely to be incompatible with the energetic of Sgr A East as constrained by Chandra [9] and HESS [12] observations. Here we only use HESS observations to normalise the primary spectrum of nuclei accelerated in Sgr A East assuming that this spectrum remain unchanged up to UHEs. Although our prediction for the EeV neutron flux is much lower than than estimated in [7] we show that such a flux should however be detectable by AUGER. In Sec.9 we summarise our conclusions.

2 Physical conditions in the Sgr A East region

Sgr A East has been observed at several wavelengths. Its distance has been determined to be $d \simeq 8$ kpc [18].

In the radio this object appears in the form of a non-thermal shell of ellipsoidal shape. The major axis of the ellipse has a length of about 10 parsecs and runs almost parallel to the galactic plane. The East side of the shell is expanding through the dense molecular cloud M-0.02-0.07 . The compressed dust/molecular ridge produced by the interaction of these objects give rise to a OH maser emission . Yusuf-Zadeh et al. [3] found some evidence of Zeeman splitting in the spectrum of this emission and inferred a magnetic field strength of 2-4 mG. Even if such a high field strength is not representative of the entire cloud, the synchrotron loss time of relativistic electrons must be considerably smaller than Sgr A East age implying that particle acceleration is still active in that region.

Detailed Far InfraRed (FIR) and Medium InfraRed (MIR) observations of the GC region have also been performed allowing to identify several diffuse and point-like sources. Here we are mainly interested in the diffuse radiation. In the Nuclear Bulge ($R \lesssim 300$ pc) the IR background appears to be dominated by cold dust emission with temperature $T \sim 20 - 50$ K (FIR). This is the true black-body emission as, in the few central parsecs of the

Galaxy, and especially in the dense Sgr A East dust ridge, the optical depth is much smaller than unity so that the intense UV radiation from the hot stars present in that region is effectively thermalised. Warm dust emission with temperature up $\sim$ 200 K dominates only in the central parsec of the Galaxy. According to the work of Davidson [19] $T \sim 40$ K for $R \sim 8$ pc and $T \sim 50$ K for $R \sim 1$ pc (see also [10, 11]). Therefore 40 K must be the temperature in the NE side of Sgr A East shell. This is also the temperature which, according to Gordon at al. [20], is typical for the molecular clouds in the Nuclear Bulge.

The spectacular Chandra [9] X-ray observations, in the energy range $2-10$ keV, with an angular resolution better than 1", confirmed that Sgr A East is the remnant of a single type II SN with age between 10^4 and 10^5 years. The total luminosity ($\sim 8 \times 10^{34}$ ergs s^{-1} in the Chandra energy range) and the spectrum of this source allowed to establish that its progenitor was a main sequence star of mass of $13-20\ M_\odot$ with a metallicity four times larger than that of the Sun. The energy of the X-ray emitting plasma was estimated to be 10^{49} ergs, which is compatible with a total kinetic energy released in the explosion of 10^{51} ergs, as for a standard type II SN. The X-ray emission is concentrated in the central ~ 2 pc of the remnant while no emission has been seen coming from the radio shell.

These observations are compatible with the theoretical predictions for a typical SNR of that age which is expected to be in an advanced cooling phase. Since the non-thermal radio shell still exists, its present velocity must be faster than the sound velocity in the ambient material. According to the authors of [9] this implies that the temperature of the ionised gas halo surrounding Sgr A East is substantially smaller than 70 K which is consistent with the IR observations. The density of the gas halo is about 10^3 cm^{-3} and it is almost homogenous barring the molecular cloud M-0.02-0.07 where it becomes as large as 10^5 cm^{-3} [21]. This dense material is swept up by the expanding shell giving rise to a thick snowplough in the form of a dust ridge surrounding the shell. The dust ridge is substantially denser at the eastern edge, where Sgr A East is interacting with the cloud, giving rise to detectable molecular line emission (molecular ridge) [21].

Soft X-ray and UV and optical radiation are effectively absorbed in such a dense medium. Even outside this opaque ridge, the flux of UV and X-ray photon density in the surrounding of the radio shell is much smaller than the IR radiation density. Indeed, the density of UV photons required to explain the gas ionisation in the GC circumnuclear disk has been estimated to be $\lesssim 10^4$ cm^{-3} [22]. An even smaller photon density has to be expected over most of Sgr A East region. The X-ray luminosity of Sgr A East observed by Chandra implies a negligible photon density over most of such SNR. The

ionising source of the gas halo surrounding the GC was not identified by Chandra. According to the authors of [9] this source may be related with a past activity of the super-massive black-hole in Sgr A* being presently in a quiescent phase. The milliGauss field strength measured by Yusuf-Zadeh et al. [3] in the Eastern side of Sgr A East may be explained by the adiabatic compression of the pre-existing field with an intensity $B_{\rm GC} \sim 10 - 100$ μG . Polarimetric observations [23], which mapped the projected magnetic field direction in the Sgr A region, support this scenario. Therefore we think it is reasonable to assume a magnetic field strength of few milliGauss in the molecular ridge crossing M-0.02-0.07, and an order of magnitude smaller field in the rest of Sgr A East non-thermal shell. The field coherence length should be several parsecs in both cases.

For what concerns particle acceleration, the weaker field present in the latter region is compensated by the larger velocity of the western shell. Indeed, the theoretically predicted shock velocity in the gas halo is $v_s \sim 6 \times 10^7$ $(t/5 \times 10^4 {\rm yr})^{-0.6}$ cms^{-1} [2] while it is expected to be few times smaller in the 10^5 cm^{-3} dense molecular cloud. Barring the effect of energy losses, the maximal CR acceleration energy should be, therefore, roughly the same over most of the Sgr A East radio shell. However, hadronic scattering in the high density cloud should prevent nuclei acceleration up to the EeV by taking place in that region. Acceleration up to the EeV may be also prevented in the South-West arc, less than 1 pc away from the GC, owing to pair production and nuclei PD energy losses (see below) onto the ~ 100 K temperature IR background present in that region.

3 Gamma rays from the GC

Several experiments observed a γ-ray excess in the direction of the GC.

EGRET satellite [24] detected an excess centred on the GC with an uncertainty of 0.2^o, corresponding to a projected lenght of 30 pc at the GC distance. In the last few years several Cherenkov telescopes allowed to explore the GC emission at higher energies. WHIPPLE [25] and CANGAROO II [26] telescopes, also found a γ-ray excess in direction of the GC in the energy range $0.2 - 1$ TeV. However, the angular resolution reached by these instruments was not much better than EGRET. A breakthrough came only recently with the HESS telescope which, thank to its stereo-graphic shower reconstruction technique, succeeded observing the GC emission up to 10 TeV with an angular resolution of 1' [12]. The background-subtracted differential flux measured by HESS is $F(E) \simeq (2.76 \pm 0.33) \times 10^{-15} (E/1 \text{ TeV})^{-2.2}$ cm^{-2}s^{-1}GeV^{-1} in the energy range 165 GeV $-$ 6 TeV [12]. The angular distribution of the

signal is compatible with a source of size < 7 pc (95% C.L.), at the distance of the GC, centred on a point that, within errors, may coincide either with Sgr A* or with the centre of Sgr A East remnant. The spectra observed by EGRET and HESS can hardly be connected so that the sources responsible for the two signals are probably different. Since the excess observed by EGRET is within the field of view of HESS but is not observed by that telescope, the source responsible for the EGRET signal (3EG J1746-2851) must be very faint above 100 GeV. For these reasons we do not consider 3EG J1746-2851 as a probable site for the acceleration of CRs up to ultra high energies.

Several sources have been proposed to be responsible for the excess observed by HESS. Among them there are the super-massive black hole in Sgr A*, in the galactic dynamical centre, a clumped halo of annihilating supersymmetric dark matter in the GC and Sgr A East. In our opinion, Sgr A East is the most plausible source for the following reasons: a) the spectrum of the GC emission observed by HESS is very similar to that of several other SNRs as measured by HESS itself and by other Cherenkov telescopes; b) no evidence of a high-energy cutoff was found up to 6 TeV which disfavours the dark matter related interpretation of the HESS signal; c) the γ-ray angular distribution detected by HESS is slightly Eastwards elongated (see Fig.1 in [12]); d) the γ-ray flux is compatible with the theoretical estimate based on the assumption that such radiation is a secondary product of hadronic cosmic rays accelerated in a SNR with the same properties of Sgr A East.

Due to the relevance of the last issue for the aims of this paper we summarise here the main passages of such computation.

Similarly to what done in [27, 7] for 3EG J1746-2851, we assume that the high energy γ-rays detected by HESS from the direction of the GC are generated by the hadronic scattering of high energy nuclei (mainly protons) accelerated by Sgr A East onto the ambient gas nuclei (mainly hydrogen). The relevant process is $pp \rightarrow pp \, + \, \mathrm{n}_\pi \pi^{\pm,0}$ (n_π is the pion multiplicity) with the neutral pions decaying into photons. At high energies the differential pp cross section can be approximated by a scaling form [28] and the photon emissivity can be written [29, 27, 7]

$$Q_\gamma(E_\gamma) \simeq n_p(E_\gamma) \sigma_{pp}^{\mathrm{ine}}(E_0) c \, n_H Y_\gamma(\alpha) \; , \tag{1}$$

where $Y_\gamma(\alpha)$ is the so-called 'spectrum-weighted moment', or 'yield', of secondary photons. In our case $Y_\gamma(2.2) = 0.103$ [29, 7]. Reasonably, the mean gas density in the Sgr A East region will not differ too much from that of the ionised gas halo surrounding the GC which, according to Chandra observations, is $\sim 10^3$ cm^{-3} (while the gas density is larger than this value in

the molecular/dust ridge, behind the shell it is smaller). We assume equipartition between the total energy of the relativistic particles accelerated by Sgr A East and the thermal energy of the X-ray emitting plasma which is amounting to 10^{49} ergs [9]. Then, by assuming a power law proton spectrum, $N_p(E) = N_0 \left(\frac{E}{E_0}\right)^{-\alpha}$, and imposing the normalisation condition

$$E_{\rm RC} = \int_{E_0}^{\infty} dE\ E N_p(E) = \frac{1}{\alpha - 2} N_0 E_0^2 \ . \tag{2}$$

we find that, for $\alpha = 2.2$ and $E_0 = 1$GeV, the expected γ-ray flux reaching the Earth is

$$F_\gamma(E_\gamma) \simeq 5 \times 10^{-15} \left(\frac{E_\gamma}{1\ {\rm TeV}}\right)^{-2.2} \left(\frac{n_H}{10^3\ {\rm cm}^{-3}}\right) \left(\frac{E_{\rm CR}}{10^{49}\ {\rm ergs}}\right) {\rm GeV}^{-1}{\rm cm}^{-2}{\rm s}^{-1} \ . \tag{3}$$

This is less than a factor two larger than the flux measured by HESS which, by accounting for the large uncertainties in the quantities involved in this computation, amounts to an excellent agreement between the model predictions and the observations.

We conclude this section by observing that TeV γ-ray attenuation due to pair-production scattering onto the IR photon background in the Sgr A East region is negligible. The mean IR photon energy is, in fact, $3kT \sim 10^{-2} \left(\frac{T}{40\ K}\right)$ eV, implying a γ-ray threshold energy of about 20 TeV. The effect may be significant only in that portion of Sgr A East shell which is within 1 pc from the GC where $T \sim 100$ K. Gamma-ray scattering onto the UV and X-ray backgrounds present in that region was also showed to give rise to a negligible attenuation [7].

4 Maximal energies of nuclei

4.1 Acceleration time scale

In the first order Fermi acceleration process, the acceleration time scale coincides with the mean time taken by a particle to cycle through the shock [2]. This is roughly given by

$$t_{\rm acc}(E) \simeq \frac{4}{c} \frac{D(E)}{u_S} \tag{4}$$

where $D(E)$ is the diffusion coefficient and u_S is the shock velocity. When the particle energy is very high it is reasonable to assume Bohm like diffusion

giving the minimum value of the diffusion coefficient $D(E) = \frac{1}{3} c R_L(E)$. The Larmor radius of a nucleus with charge Z is

$$R_L(E) = \frac{E}{Z\ eB} \simeq \frac{1}{Z}\ 10\ \left(\frac{E}{10^{18}\ \mathrm{eV}}\right)\left(\frac{B}{100\ \mu\mathrm{G}}\right)^{-1}\ \mathrm{pc}\ . \qquad (5)$$

An important condition to be fulfilled is that $R_L(E_{\max})$ does not exceed the size of the SNR.

Using the previous expressions we find

$$t_{\mathrm{acc}}(E) \sim \frac{1}{Z}\left(\frac{E}{10^{18}\ \mathrm{eV}}\right)\left(\frac{B}{100\ \mu\mathrm{G}}\right)^{-1}\ \left(\frac{u_S/c}{10^{-3}}\right)^{-1}\ 10^{12}\ \mathrm{s}\ . \qquad (6)$$

Nuclei acceleration up to UHEs might be prevented by one of the following processes: a) hadronic collisions onto the gas particles; b) electron-positron pair-production by the interaction with low energy photons; c) photo-disintegration onto background photons. The relative relevance of these processes depends on the physical conditions in the acceleration region.

4.2 Energy losses due to hadronic collisions

The gas density in the GC region is considerable larger than the mean ISM density. Chandra observations [9] allowed to infer that Sgr A East shell is expanding through a ionized gas halo with mean density $n_H \sim 10^3$ cm^{-3}. The hydrogen density can be as high as $\sim 10^5$ cm^{-3} in the molecular cloud M-0.02-0.07 . The nucleus-proton scattering time scale is

$$t_{\mathrm{hadr}} \simeq \frac{1}{A^{2/3}\ c n_H K \sigma_{pp}} \simeq A^{-2/3}\ 10^{12}\ \left(\frac{n_H}{10^3\ \mathrm{cm}^3}\right)^{-1}\ \mathrm{s}\ , \qquad (7)$$

where the pp cross section $\sigma_{pp}(E)$ and the inelasticity K are given in the Appendix. The $A^{2/3}$ factor in (7) is due to the grown of the effective surface taking part to the pA interaction respect to the pp scattering. We can safely neglect here the weak energy dependence of σ_{pp} and K. A more detailed treatment will be performed while determining the spectrum of the secondary particles produced by the pp scattering (see Sec.6).

4.3 Pair-production energy losses

As we discussed in Sec.2 the region where Sgr A East is located is pervaded, besides by the hydrogen gas, by a background of black-body radiation at a

temperature ~ 40 K. Therefore, the photon density in that region is considerably larger than in the interstellar and intergalactic media where the CMB is the dominant radiation background. It is well known in cosmic ray physics that a photon background give rise to significant energy losses of UHECRs. Besides the PD, which in our case is a useful process and will be considered in Sec.5, the most relevant loss process for nuclei is the pair production: $((A,Z)\gamma \to (A,Z) + e^+e^-)$. This process has been studied in details in two seminal papers by Blumenthal [30] and Chodorowsky et al. [31]. Applying the results found in those papers we find

$$\begin{aligned} t^{-1}_{\rm pairs} =& \frac{2\alpha r_0^2}{\pi^2 c^{\,2}\hbar^3}\frac{Z^2}{A}\frac{m_e}{m_p}(kT)^3 f(\gamma T) \\ =& \frac{Z^2}{A} f(\gamma T)\left(\frac{T}{40\ {\rm K}}\right)^3\ 1.4\times 10^{-15}\ {\rm s}^{-1} \end{aligned} \tag{8}$$

where $\gamma = E/Am_N$. The function

$$f(\gamma T) = \left(\frac{m_e c^2}{\gamma k T}\right)^3 \int_2^\infty d\xi\ \phi(\xi)\frac{1}{e^{\frac{\xi m_e c^2}{2\gamma k T}}-1}\ , \tag{9}$$

where $\phi(\xi)$ is defined in [31], is plotted in Fig. 1.

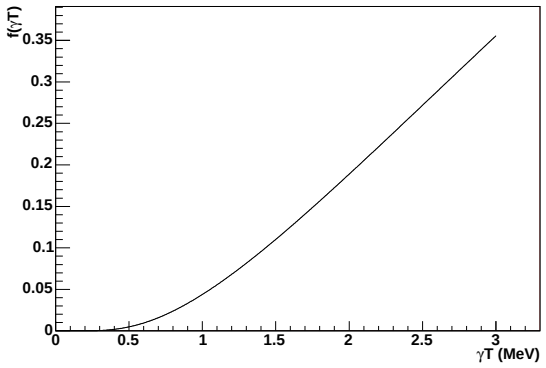

Figure 1: The function $f(\gamma kT)$ is represented.

Therefore, it follows from Eq.s (8) and (7) that in Sgr A East pair-production losses of ultra-relativistic nuclei are subdominant respect to hadronic losses. Photo-pion production also does not play any significant role in the energy range of interest for this work.

4.4 Maximal energy

An order of magnitude estimate of the maximal energy reachable by diffusive shock acceleration can be determined by imposing the condition

$$t_{\rm acc}(E) = \min\left\{t_{\rm loss}(E),\ t_{\rm SNR}\right\}\ , \tag{10}$$

where $t_{\rm acc}(E)$, $t_{\rm loss}(E)$ and $t_{\rm SNR}$ are respectively the characteristic acceleration time, energy loss time and the age of the SNR. As we showed in the above, energy losses in the Sgr A East region are dominated by hadronic scattering with a characteristic time given by Eq. (7). Sgr A East age is

$$t_{\rm SgrAEast} \sim 5 \times 10^4 \text{ yr} \simeq 10^{12} \text{ s}\ . \tag{11}$$

which, especially for heavy nuclei, is larger than $t_{\rm hadr}$.

Therefore by substituting (6) and (7) into (10) we find that the maximal energy reachable by shock acceleration in Sgr A East is roughly given by

$$E_{\rm max} \simeq\ \frac{Z}{A^{2/3}}\ \left(\frac{u_S/c}{10^{-3}}\right)\left(\frac{B}{100\ \mu\text{G}}\right)\ \ 10^{18}\text{ eV}\ . \tag{12}$$

We conclude that the acceleration of nuclei up to the ankle of the CR spectrum in Sgr A East is plausible. According to Croker *et al.*, even larger energies may be reached in that object if the magnetic field has a component non-perpendicular to the shock.

5 Neutron production by nuclei photo-disintegration onto the IR background

To determine the production rate of neutrons by the photo-disintegration (PD) of high energy nuclei interacting with a heat bath of photons we apply the results of Puget, Stecker and Bredekamp [32]. Following what done in [32], the photo-disintegration rate for a nucleus of atomic number A (we consider only stable nuclear species) releasing i nucleons can be written as

$$R_{A,i} = \frac{1}{2\gamma^2}\int_0^\infty d\epsilon\epsilon^{-2}n(\epsilon)\int_0^{2\gamma\epsilon} d\epsilon'\epsilon'\sigma_{A,i}(\epsilon') \tag{13}$$

where γ is the Lorentz factor of the nucleus, and ϵ, ϵ' the photon energy in the observer and nucleus rest frames respectively. In general, the PD cross section is well approximated by the sum of two terms: a term describing one- and two-nucleon PD, which is dominated by the giant dipole resonance, and

a non-resonant term which is relevant for the multi-nucleon emission only. For $\gamma kT \ll 30$ MeV, which is the case in the present context, the latter term gives a negligible contribution. The function

$$\sigma_{A,i}(\epsilon') \simeq \sum_{i=1}^{2} \theta(\epsilon' - \epsilon^{\rm th}_{A,i})\theta(30\ {\rm MeV} - \epsilon')\ W^{-1}_{A,i}\xi_{A,i}\Sigma_d \exp\left[-\left(\frac{\epsilon' - \epsilon'_{o\ A,i}}{\Delta_{A,i}}\right)^2\right] \tag{14}$$

was found to provide a good fit of the experimental data [32]. The definitions of the parameters $\epsilon^{\rm th}_{A,i}$, $\epsilon'_{0,i}$, $\Delta_{A,i}$ and $\xi_{A,i}$ are given in [32, 33]. In Tab.1 we report their values for the PD of most abundant nuclides with the emission of only one nucleon. For the threshold energies $\epsilon^{\rm th}_{A,i}$ we use the values given in Stecker and Salamon [33] which we also report in the same table. The strength of the PD reaction, i.e., the integral of cross section over the relevant energy interval, is $\Sigma_d = \dfrac{(A-Z)Z}{A} 5.98 \times 10^{-26}$ MeVcm^2. The normalisation constant is given by

$$W_{A,i} = \sqrt{\frac{\pi}{8}}\left[{\rm erf}\left(\frac{30\ {\rm MeV} - \epsilon'_{0,\ A,i}}{\Delta_{A,i}/\sqrt{2}}\right) + {\rm erf}\left(\frac{\epsilon'_{0\ A,i} - \epsilon^{\rm th}_{A,i}}{\Delta_{A,i}/\sqrt{2}}\right)\right]\ . \tag{15}$$

Nuclear species	A	Z	$\epsilon^{\rm th}_1$	$\epsilon'_{0\ 1}$	Δ_1	ξ_1
Fe	56	26	11.2	18	8	0.98
O	16	8	15.7	24	9	0.83
C	12	6	18.7	23	6	0.76
He	4	2	20.6	27	12	0.47

Table 1: PD cross section parameters for the most abundant nuclides as given in [32, 33]. The ϵ's and Δ are in MeV.

We find convenient to express the photo-disintegration rate in the form:

$$R_{A,i}(\gamma T) \simeq R_0\ \xi_{A,i}\left(\frac{T}{40\ {\rm K}}\right)^3 \Phi_{A,i}(\gamma T) \tag{16}$$

where

$$R_0 = \frac{1}{2\pi^2\hbar^3c^2}\ (5.98 \times 10^{-26}\ {\rm cm}^2)\ (k\ 40\ {\rm K})^3 \simeq 5 \times 10^{-10}\ {\rm s}^{-1}\ . \tag{17}$$

The function $\Phi_{A,i}$ is defined by

$$\Phi_{A,i}(x) \equiv (W\Delta)^{-1}_{A,i}\ \frac{(A-Z)Z}{A}\ x^{-3} \int_{\epsilon^{\rm th}_{A,i}}^{15\ {\rm MeV}} d\tilde{\epsilon}\left(e^{-\tilde{\epsilon}/x} - 1\right)^{-1} J_{A,i}(\tilde{\epsilon})\ , \tag{18}$$

where

$$J_{A,i}(\tilde{\epsilon}) \equiv \int_{\epsilon_{A,i}^{\rm th}}^{2\gamma\tilde{\epsilon}} dy\ y \exp\left\{-2\left(\frac{y-\epsilon'_{0\ A,i}}{\Delta_{A,i}}\right)^2\right\}\ . \tag{19}$$

We verified that further contributions to the PD rate which were considered in [32] are subdominat in our case.

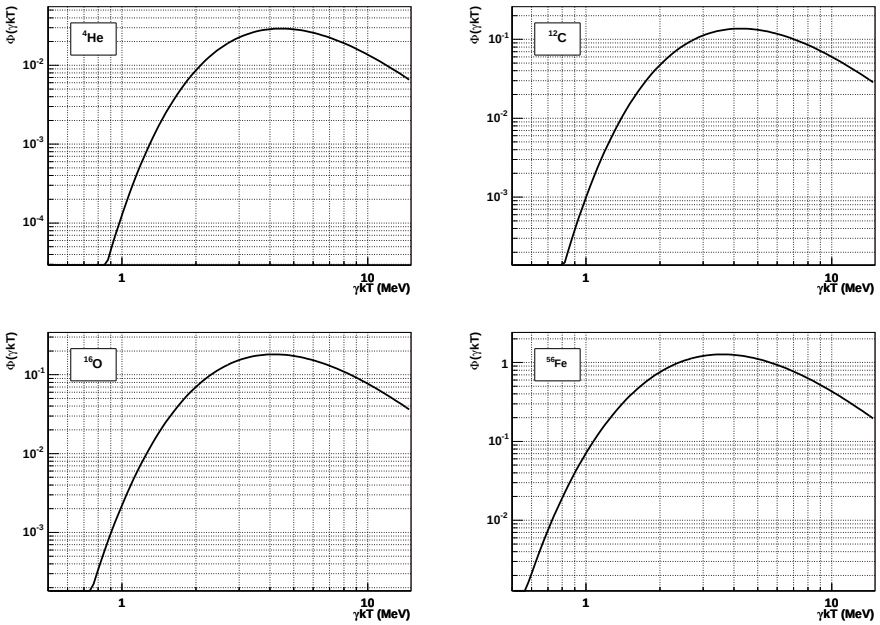

Figure 2: The function $\Phi_{A,1}(\gamma kT)$ is represented for ^{4}He, ^{12}C, ^{16}O and ^{56}Fe.

In Fig. 2 we represent the function $\Phi_{A,1}$ for several nuclear species. Interestingly, we found that for all relevant nuclei the photo-disintegration rate is peaked at $\gamma kT \approx 4$ MeV. We will see that this property has relevant consequences for the spectrum of the secondary neutrons. In terms of the nucleus energy the peak condition reads

$$E_A^{\rm peak} \simeq A \times 10^{18}\ \left(\frac{T}{40\ {\rm K}}\right)^{-1}\ {\rm eV}\ . \tag{20}$$

The maximal value of $\Phi_{A,i}$ is different for different nuclear species. We consider here only those species which are expected to have the largest abundance in Sgr A East. The reader can see from Fig.2 that, among the most abundant elements, iron (^{56}Fe) nuclei have the highest maximal value of the PD rate. However, due to grow of energy losses with A (see Eq.7), we do not

expect heavy nuclei to reach $E_A^{\rm peak}$. Furthermore, even disregarding hadronic energy losses, a too rapid PD (note that the maximal PD rate of ^{56}Fe is much larger than the inverse age of Sgr A East) would itself prevent Iron nuclei reaching $E_A^{\rm peak}$. This is not the case for ^{4}He nuclei having a PD peak rate which is almost coincident with the inverse of the Sgr A East age. We assume here that the physical conditions in Sgr A East (namely the local magnetic field intensity and geometry nearby the shock) allow the acceleration of ^{4}He nuclei up to few EeV, corresponding to a value of Φ_4 of $(2 \div 3) \times 10^{-2}$. As we showed in Sec. 4 such conditions are not unrealistic.

In order to evaluate the flux of secondary neutrons reaching the Earth we need to estimate the relative abundance of the main nuclear species in the SNR shell. Since we are assuming that all nuclei are accelerated by the same mechanism under the same physical conditions, we expect them to share the same power-law spectrum, namely $N_A(E) = f_A N_0 \left(\frac{E}{E_0}\right)^{-\alpha}$, where f_A parametrizes the relative abundance of nuclear species in the SNR shell. Although, as we discussed in Sec.4, the spectra of different nuclear species may have different UV cut-off energies, for $\alpha > 2$ this has no significant effect on the CR energetic. N_0 can be readily determined by imposing the normalisation condition (2).

Assuming a uniform cosmic ray density in the acceleration region, the neutron emissivity is therefore

$$Q(E_n) = \frac{1}{2\,V} \sum_A \sum_{i=1}^{2} i f_A (\alpha - 2) E_{\rm CR} \left(\frac{A E_n}{E_0}\right)^{-\alpha} \min\left\{R_{A,i},\ t_{\rm SNR}^{-1}\right\} \qquad (21)$$

where $m_N = (m_p + m_n)/2$ and V is the volume of the emitting region. We assumed a probability 1/2 for the expelled nucleon to be a neutron. We used here that any neutron expelled during the photo-disintegration carries, in average, a fraction $1/A$ of the parent nucleus energy. The two nucleon emission process is subdominant and we neglegt it in the following. The minimum condition in (21) is required since for $R_A(\gamma T) > t_{\rm SNR}^{-1}$ any further acceleration is effectively inhibited by the PD energy losses.

According to Chandra observations, Sgr A East metallicity is about four time that of the Sun. As a consequence we estimate the iron/hydrogen relative abundance to be $f_{56} \simeq 10^{-3}$. The PD condition ($R(56) \sim t_{\rm SNR}^{-1}$) is reached for $\gamma kT \sim 0.7$ MeV corresponding to a neutron energy $\sim 2 \times 10^{17}$ eV. Carbon and Oxigen should have a comparable abundance and a smaller peak rate so that their PD gives rise to neutrons of energy $\sim$ few $\times 10^{17}$ eV. These neutrons however are hardly detectable due to their smaller time-life and the small abundance of the corresponding primary nuclei. The most significant contribution to the neutron flux reaching the Earth should come from the

PD of ^{4}He nuclei. Indeed $f_4 \simeq 0.1$ in Sun, and it is presumably even larger in the remnant of a type II SN (unfortunately ^{4}He is quite difficult to observe). Furthermore, as we showed in the above, for the ^{4}He the PD condition is reached just at the energy where the PD rate takes its maximal value so that, as follows from Eq. (20), the flux of secondary neutrons will peak at the energy

$$E_n^{\rm peak} \simeq \frac{E_A^{\rm peak}}{A} = 1 \times 10^{18} \ \left(\frac{T}{40 \ {\rm K}}\right)^{-1} \ {\rm eV} \ . \tag{22}$$

This is just the energy required for the neutron flux to be not suppressed significantly by the decay on the way from the GC to the Earth.

Using (21) and accounting for the finite lifetime of neutrons we finally find that for $\alpha = 2.2$ the expected neutron flux reaching the Earth from Sgr A East is

$$\frac{dF(E_n)}{dE_n} \simeq 2 \times 10^{-27} \ \left(\frac{f_A}{0.1}\right) \left(\frac{R_0 \xi_A \Phi_A(E_n, T)}{10^{-12} \ {\rm s}^{-1}}\right) \left(\frac{E_{\rm CR}}{10^{49} \ {\rm ergs}}\right) \left(\frac{d}{8 \ {\rm kpc}}\right)^{-2} \left(\frac{T}{40 \ {\rm K}}\right)^{3} \exp\left(-\frac{d \ m_n}{E_n \ c\tau_n}\right) \left(\frac{A E_n}{10^9 \ {\rm GeV}}\right)^{-2.2} \ {\rm GeV}^{-1}{\rm cm}^{-2}{\rm s}^{-1} \ . \tag{23}$$

Note that, since the neutron mean time-life is $\tau_n = 887$ s [34], the neutron survival probability for $E_n = 10^{18}$ eV and $d = 8$ kpc is $P_{\rm sur} = \exp\left(-\frac{d \ m_n}{E_n \ c\tau_n}\right) \simeq 0.43$.

The spectrum of neutrons produced by the PD of ^{4}He nuclei is represented in Fig.3. While below 1 EeV the flux is exponential suppressed due to the combined effect of the PD threshold and the neutron decay, above that energy the neutron spectrum is a power-law of index ~ 5 as an effect of the convolution of the primary nuclei spectrum with the E^{-3} high energy behaviour of the PD rate. The value $f_4 = 0.1$ was assumed drawing Fig.3. This is a quite conservative assumption, as the relative ^{4}He abundance in Sgr A East is likely to be few times larger.

We conclude this section by observing that PD of ^{4}He nuclei onto the UV and X-ray backgrounds in the surrounding of Sgr A East cannot prevent their acceleration up to UHEs. In fact, in Sec.2 we argued that the number density of photons in that energy range is $n_{\rm UV} \simeq n_X \lesssim 10^4$ cm^{-3}. This is smaller than the photon density of the IR background at 40 K by more than two orders of magnitude. We showed in the above, that the PD rate does not depend on the absolute value of the nucleus energy but only on the product of its Lorentz factor with the photon energy. As a consequence, the maximal PD rate due to UV and X-ray is the same of (16) but for the re-scaling factor

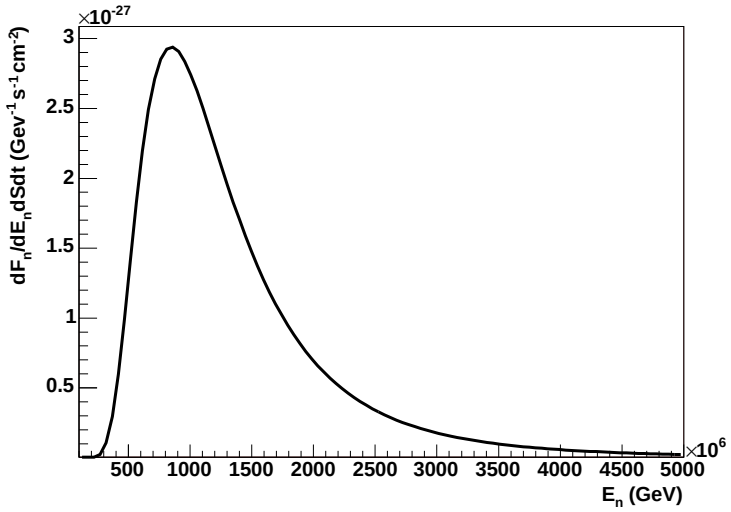

Figure 3: The differential flux reaching the Earth of neutrons produced by the photo-disintegration of ^{4}He nuclei in Sgr A East

$n_{\rm UV,\ X}/n_{\rm IR} \simeq 10^{-2}$. In the case of ^{4}He nuclei this quantity is smaller than Sgr A East age by the same amount.

6 Neutrons from pp collisions

Besides the PD process discussed in the previous section, EeV neutrons might be also be produced by the collision of UHE nuclei with the dense gas in the GC environment. The relevant neutron production channel is the charge exchange pp inelastic collision $pp \to pn + {\rm n}_\pi\pi$, where ${\rm n}_\pi$ is the pion multiplicity.

The neutron emissivity is

$$Q_n^{pp}(E_n) = c\, n_H \int_{E_{th}(E_n)} dE_p\, n_p(E_p) \frac{d\sigma^{\rm inel}(E_n, E_p)}{dE_n} \qquad (24)$$

where $\dfrac{d\sigma_{pp}^{\rm inel}(E_n, E_p)}{dE_n}$ is the pp differential inelastic cross section. This quantity is experimentally undetermined for E_p larger than few hundred GeVs. We handle this problem by combining Monte Carlo simulations with an analytical calculation based on the scaling properties of the differential cross section at high energy. In the Appendix we find

$$Q_n^{pp}(E_n) = c\, n_H n_p(E_n) \sigma_0 0.24\, \frac{4}{5} \left[I_1(\alpha) + I_2(\alpha) \ln\left(\frac{E_n}{E_0}\right) \right] \qquad (25)$$

where $\sigma_0 \equiv \sigma_{pp}(E_0)$ and the functions $I_1(\alpha)$ and $I_2(\alpha)$ are given in (38).

Respect to a similar approach followed by the authors in [7], our scaling function provides a better fit of the MC data at high values of E_n/E_p and takes properly into account the grown of the cross section at very high energies. As we did in the previous sections we assume here that the energy spectrum of protons accelerated by the SNR is a power law of index α.

Then, by assuming $\alpha = 2.2$ and accounting for the finite lifetime of the neutron, we find that the differential neutron flux due to *pp* scattering which should reach the Earth is:

$$F_n(E_n) \simeq 8 \times 10^{-28} \left(\frac{E_n}{1\ \mathrm{EeV}}\right)^{-2.2} \left(\frac{n_H}{10^3\ \mathrm{cm}^{-3}}\right) \left(\frac{E_{\mathrm{CR}}}{10^{49}\ \mathrm{ergs}}\right) \left(\frac{d}{8\ \mathrm{kpc}}\right)^{-2} \exp\left(-\frac{d\ m_n}{E_n\ c\tau_n}\right)\ \mathrm{GeV}^{-1}\mathrm{cm}^{-2}\mathrm{s}^{-1}\ . \quad (26)$$

This is represented in Fig.4.

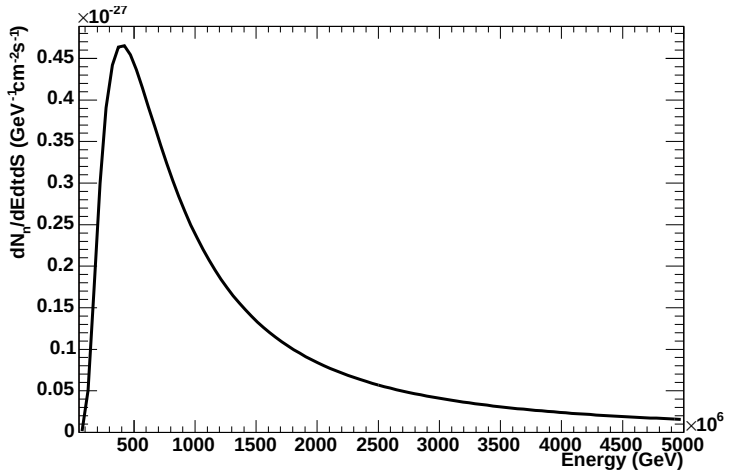

Figure 4: The differential flux reaching the Earth of neutrons produced by *pp* collisions.

A comment is in order here. In the appendix we showed that the mean value of the neutron elasticity ($\langle x \rangle \equiv \langle E_n/E_p \rangle$) is ~ 0.05. Therefore, the maximal proton energy must be larger than 2×10^{19} eV to give rise to unsuppressed neutron flux. In the derivation in the above we didn't account for a UV cut-off in the proton energy spectrum implicitly assuming that this is far above the EeV. This assumption, however, is probably unrealistic even

for Sgr A East (see Sec.4). As a consequence, a suppression of the neutron flux due to pp scattering has to be expected respect to the estimate given in (26) unless Sgr A East is an extremely energetic proton accelerator.

7 Expected signal at AUGER

The Pierre AUGER Observatory is an Extensive Air Shower detector under construction in Argentina [13]. When completed, it will consist of 1600 Water Cherenkov elementary Detectors (WCDs) covering an area of about 3000 km^2 overlooked by a set of four florescence telescopes. An Engineering Array of WCDs has been in operation since 2002 and the detection of several showers with energy of the primary $\sim 10^{18}$ eV has already announced at the ICRC 2003 [35]. The AUGER acceptance will be $A\Omega \approx 4700$ km^{2}sr, for a zenith angle $\theta < 45^o$. The array trigger efficiency at the EeV has been estimated to be $\eta \simeq 0.25$ [35].

The geographic position of AUGER is ideal for observing a UHECR excess in the direction of the GC. Since the angular size of Sgr A East is few primes, the neutron emission from this object should give rise to a point-like signal in AUGER. [1] More precisely, the expected signal should be seen under the form of a CR excess in the angular bin corresponding to the position of the source. The angular bin covers a solid angle $\omega = \pi\delta^2$, where δ is the angular resolution of the detector. The AUGER angular resolution δ is expected to be around 1^o at $10^{19} - 10^{20}$ eV (implying $\omega \simeq 1 \times 10^{-3}$ sr) but it δ will probably be $2^o - 3^o$ (in the final configuration) around the EeV [13].

The isotropic background of ordinary CRs gives rise to an unavoidable noise. The CR spectrum in the energy range $4 \times 10^{17} < E < 6.3 \times 10^{18}$ eV is [38]

$$J_{\rm CR}(E) = (9.23 \pm 0.65) \times 10^{-28} \left(\frac{E}{6.3 \times 10^{18}}\right)^{-3.20\pm0.05} \ (\text{GeV sr cm}^2\ \text{s})^{-1} \ . \tag{27}$$

Therefore the maximal (at 95%C.L.) differential flux around 10^{18} eV incident onto the expected AUGER angular bin is

$$F_{\rm CR}^{\rm max}(E) \simeq 3 \times 10^{-27} \left(\frac{E}{10^{18}\ \text{eV}}\right)^{-3.3} \ \left(\frac{\delta}{2.5^o}\right)^2 \ \text{GeV}^{-1}\text{cm}^{-2}\text{s}^{-1} \ . \tag{28}$$

It is comforting that the expected neutron flux from Sgr A East produced by the photo-disintegration of ^{4}He nuclei (see Eq. 23) is comparable to the

[1] In principle, EeV protons produced nearby the Earth by neutron decay may give rise to a smeared signal superimposed to the point-like excess [36, 37]. This secondary signal, however, is probably undetectable.

isotropic CR flux around the EeV incident over the AUGER angular bin. As a consequence, AUGER may observe a significant UHECR excess in the angular bin corresponding to the position of the GC.

As a benchmark, we give here the expected rates of showers incident over an angular bin of 2.5^0, in the energy range $1 \times 10^{18} < E < 3 \times 10^{18}$ eV, due to the PD and *pp* neutrons respectively (accounting for the AUGER trigger efficiency)

$$\dot{N}_{\rm PD} \simeq 132 \ {\rm yr}^{-1} \quad \dot{N}_{pp} \simeq 72 \ {\rm yr}^{-1} \ , \tag{29}$$

$\dot{N}_{\rm PD}$ has been computed assuming the ^{4}He relative abundance $f_4 = 0.2$ (see the discussion at the end of Sec.5). These rates have to be compared with a CR background rate in the same angular and energy bins which is

$$\dot{N}_{\rm CR} \simeq 440 \ {\rm yr}^{-1} \ . \tag{30}$$

Since the expected signal is a sizeable fraction of the background a significant excess should be detectable in the direction of the GC.

We conclude that, under the conditions that we assumed in this paper, the signal due to EeV neutrons produced by Sgr A East should not be missed by AUGER.

8 Discussion

The possibility, discussed in this paper, of testing if nuclei acceleration takes place in Sgr A East up to Ultra High Energies ($E > 10^{18}$ eV) by looking for EeV neutrons coming from the GC direction, was also considered in a recent paper by Crocker *et al.* [7]. Our work, however, differs from that of Crocker *et al.* in a number of relevant aspects.

First of all, the aim of Crocker *et al.* was to interpret the anisotropy in the CR angular distribution observed, around the EeV, by the AGASA [14] and the SUGAR [17] experiments in a direction relatively close to that of the GC. This is not our attitude. Indeed, even accepting AGASA and SUGAR results as evidences of real CR anisotropies, which is tricky due to their rather low statistical significance, it is, in our opinion, rather hazarding to identify Sgr A East as the source responsible for these signals. Indeed, neither the AGASA nor the SUGAR UHECR excesses are in the direction of the very GC. The GC is not even in the "field of view" of AGASA being below its geographic horizon. [2] While SUGAR is in the right geographic position for

[2] We have to note here that an extended signal due to the protons produced by neutron decay has to be expected [36, 37]. Although, this signal might explain the anisotropy observed by AGASA in terms of a neutron source located in the GC, the required neutron

observing the GC, no excess was observed by this experiment from the true centre of the Galaxy. The SUGAR peak was 7.5^o away from the GC and it does not even appear to be centred on the galactic plane. This offset is too large to be due to a possible systematic pointing error of the experiment. For these reasons we think that Sgr A East cannot be responsible for the AGASA and SUGAR anisotropies. It is important to notice that SUGAR was not sensitive enough to be able to detect the neutron flux which we predicted in Sec.s 5 and 6 to come from Sgr A East. Therefore, the lack of signal in the direction of the GC in the SUGAR data set does not contradict the hypothesis raised in this paper.

The normalisation of the relativistic particle spectrum in Sgr A East which was adopted in [7] was based on a combined fit of the low energy γ-ray signal observed by EGRET [24] in the direction of the GC and the AGASA/SUGAR anisotropy data. As we explained in Sec.3, and noted also by the authors of [7], the γ-ray spectrum of the source responsible for the EGRET excess cannot extend up to very high energies. It is, therefore, quite unnatural to assume that this source accelerates CRs up to the EeV. Although in [7] the authors also (marginally) consider a HESS + AGASA/SUGAR fit, in order this to work they need to adopt a power index 1.97 for the proton spectrum which is almost 3σ lower than the HESS best fit [12] (as we showed in Sec.3, the spectrum of high energy secondary photons is expected to have the same slope as that of primary protons). Such a discrepancy may become more serious if new data from HESS would prolong the GC γ-ray spectrum observed so far to even higher energies.

Last but not least, the contribution of nuclei photo-disintegration to Sgr A East neutron emission was not determined in [7]. We showed, however, that this process should provide the dominant, if not the unique, channel for the production of EeV neutrons.

In this paper we did not discuss the contribution to the synchrotron radio emission and to the inverse Compton (IC) low-energy γ-ray flux from Sgr A East which may be produced by secondary leptons. The possible relevance of these emissions was studied in [27]. The authors of [27] assumed that the γ-ray flux observed by EGRET [24] is a by-product of *pp* inelastic scattering in Sgr A East and used EGRET measurements to normalise the primary proton flux. On the basis of these assumptions, they estimated the expected radio and IC secondary fluxes showing that these emissions are compatible with the observations. Since the normalisation of the relativistic nuclei spectrum that we used in this paper (which is based on HESS observations) is much

luminosity of such source, which was determined in [37], is too high to be compatible with its possible identification with Sgr A East.

lower, we are confident that secondary emissions are even harmless in our case.

We also did not discuss here the possible effect of post-acceleration diffusion on the primary nuclei spectrum. In principle, since diffusion is an energy dependent process, deviation from a single power-law behaviour may arise in the nuclei spectrum. Some possible consequences of high energy proton diffusion in the GC region has been recently discussed in [39]. Here we implicitly assumed that above several TeV (the energy required to produce the TeV gamma-rays observed by HESS) protons spectrum around Sgr A East coincides with the acceleration spectrum.

9 Conclusions

In this paper we estimated the flux of neutrons reaching the Earth from Sgr A East under the educated hypothesis that nuclei are accelerated beyond the EeV in that SNR. We showed that neutrons with the required energy ($\sim$ 1EeV) can be naturally produced by the photo-disintegration (PD) of composite nuclei onto the IR background radiation present in the GC region and by the *pp* scattering of UHE protons onto the dense hydrogen gas surrounding Sgr A East. We found the former process to be the dominant. Amazingly, the PD rate of nuclei onto the 40 K photon background peaks just at the energy required to produce EeV neutrons which can reach the Earth from the GC before decaying. Due to their largest abundance respect to other composite nuclides, ^{4}He nuclei should give the main contribution to the neutron flux. While the energy threshold for *pp* scattering is much lower, due to the low neutron elasticity (the fraction of the primary proton energy going to the neutron) the energy required to primary protons in order to produce EeV neutrons is, in average, higher than 10 EeV. Such a high energy may be hardly reachable even in Sgr A East so that the contribution of *pp* inelastic scattering to the EeV neutron flux may be absent.

The signal produced by the EeV neutrons from Sgr A East should be easily disentangled from the CR isotropic background thanks to its particular spectrum and its point-like nature. As we showed in Sec.5, the neutron spectrum should start to rise rapidly above $few \times 10^{17}$ eV, to peak just below the EeV, and become a power law steeper than the CR spectrum at higher energy. The reader should take in mind, however, that a UV cut-off may come-in somewhere above the EeV as the maximal acceleration energy in Sgr A East cannot be indefinitely high. Presumably, only one energy bin around the EeV will be interested by the excess. The clearest signature of the neutron flux from Sgr A East should be given, however, by the point-like nature of

the excess and by its coincidence with the actual position of this SNR in the sky coinciding with that of the GC. By assuming that nuclei accelerated in Sgr A East have a power law spectrum with exponent -2.2, as suggested by HESS gamma-ray observations, and that this spectrum extend steadily beyond the EeV, we determined the flux of secondary neutrons expected to reach the Earth and showed that the Pierre AUGER Observatory should be able to detect it.

We conclude by observing that several of the results that we derived in this work for Sgr A East should also be applicable to some other SNRs. As we discussed in the Introduction, the most promising neutron/gamma-ray emitters as those SNRs interacting with dense molecular clouds. The fast improvements in gamma-ray astronomy and in the extensive air shower reconstruction techniques may allow soon a systematic search of galactic EeV-trons.

Acknowledgements

We thank F. Aharonian, P. Blasi, V. Cavasinni, S. Degl'Innocenti, E. Roulet, S. Shore and M. Vietri, for valuable discussions and in particular F.A., V.C., E.R., S.S. and M.V. for reading the draft of this paper providing several useful hints and comments. This work would not have been possible without the assistance and support of the Pisa ANTARES group. L.M. thanks G. Usai for help using the PYTHIA package.

Appendix

The pp total cross-section determined by combining collider and UHECR ($pp_{\rm air}$ scattering) data [34] is

$$\sigma_{pp}(s) = Z_{pp} + B\ \ln^2\left(\frac{s}{s_1}\right) \tag{31}$$

where $Z_{pp} = 35.48 \times 10^{-27}$ cm^2, $B = 0.310 \times 10^{-27}$ cm^2 and $s_1 = (5.38\ \text{GeV})^2$.

Clearly, we are interested only in the inelastic pp scattering. The inelasticity K is defined by $\sigma_{pp}^{\rm inel} = K\sigma_{pp}$ From the experimental data of the pp and $p\bar{p}$ scattering $K \simeq 4/5$. For $s > 10$ GeV^2 there is no evidence of a variation of K with energy.

The neutron emissivity can be written in the form

$$Q_n^{pp}(E_n) = c\ n_H \int_{E_p^{min}}^{\infty} dE_p\ n_p(E_p)\ \mathrm{n}_n \sigma_{pp}^{\rm inel} \frac{dP_n}{dE_n}(E_n, E_p)\ , \tag{32}$$

where n_n is the neutron multiplicity and $\dfrac{dP_n}{dE_n}(E_n, E_p)$ is the normalised probability distribution to produce a neutron with energy E_n.

Since neither experimental data nor undisputed theoretical calculations are available allowing to determine these quantities at UHEs, we resort to Monte Carlo simulations. We used the PYTHIA generator [40] to simulate pp inelastic scattering for several values of E_p in the range $1 - 10^3$ TeV under the constraint that the total cross section is that given in (31). We found the value of the neutron multiplicity to be $\mathrm{n}_n = 0.24$ almost independently on E_p. The simulation also allowed to determine the neutron energy distribution. Again, the result was practically energy independent meaning that differential cross section $\dfrac{d\sigma}{dE_n}$ can be written in a scaling form:

$$\frac{d\sigma}{dE_n} = \sigma_{inel}\, \mathrm{n}_n\, \frac{dP_n}{dE_n}(E_n, E_p) = \mathrm{n}_n\, \frac{\sigma_{pp}^{\mathrm{inel}}}{E_n}\, h(x)\ , \tag{33}$$

where $x \equiv E_n/E_p$. The best fit to the Monte Carlo data gives

$$h(x) \simeq 0.064\,(1-x)^2 + 0.094 x\sqrt{1-x}\ . \tag{34}$$

This result is similar to that found by Drury et al. [41] but for the last term, being absent in their work, which allow a better fit of the MC data for $x \to 1$.

The mean value of x, the so called neutron *elasticity*, is

$$\langle x \rangle = \int_0^1 dx\ h(x) \simeq 0.05\ , \tag{35}$$

Before inserting the previous results in (32) we rewrite the inelastic cross section in the form

$$\sigma_{pp}^{\mathrm{inel}}(E_p) = \sigma_0\ \left(1 + D \ln\left(\frac{E_p}{E_0}\right)\right)\ , \tag{36}$$

where we defined $\sigma_0 \equiv \sigma_{pp}(E_0) \simeq K \times Z_{pp}$, and $D \equiv 2B/Z_{pp} = 1.7 \times 10^{-2}$ where $E_0 = 1$ GeV. The neutron emissivity can then be written as

$$Q_n^{pp}(E_n) = c\, n_H n_p(E_n) \sigma_0 \mathrm{n}_\mathrm{n} K \left[I_1(\alpha) + I_2(\alpha) \ln\left(\frac{E_n}{E_0}\right)\right] \tag{37}$$

where

$$\begin{aligned} I_1(\alpha) &\equiv \int_0^1 dx\, x^{\alpha-2} h(x)(1 - D\ln(x)) \\ I_2(\alpha) &\equiv D \int_0^1 dx\, x^{\alpha-2} h(x)\ . \end{aligned} \tag{38}$$

Clearly, a regularization procedure is needed in order to avoid singularities near $x = 0$. Obviously the correct regularization is made when one considers the finite mass of the neutron, which forces the integration domain to be $\left[\frac{m_n}{E_p}, 1\right]$.

References

[1] L. O'C. Drury, Rept. Prog. Phys. **46** (1983) 973.

[2] P. O. Lagage and C. J. Cesarsky, Astron. Astrophys. **125** (1983) 249 .

[3] F. Yusef-Zadeh et al., Astrophys. J. **466** (1996) L25 .

[4] C. Heiles and R. Crutcher, arXiv:astro-ph/0501550.

[5] A. R. Bell and S. G. Lucek, Mon. Not. R. Astron. Soc. **321** (2001) 433.

[6] L. O. Drury, F. A. Aharonian and H. J. Volk, Astron. Astrophys. **285** (1994) 645 [arXiv:astro-ph/9305037].

[7] R. M. Crocker, M. Fatuzzo, R. Jokipii, F. Melia and R. R. Volkas, Astrophys. J. **622** (2005) 892 [arXiv:astro-ph/0408183].

[8] L. Sidoli, S. Mereghetti, A. Treves, L. Chiappetti, G. L. Israel and M. Orlandini, Astrophys. J. **525** (1999) 215 arXiv:astro-ph/9904393.

[9] Y. Maeda et al., Astrophys. J. **570** (2002) 671.

[10] R. Zylka et al., Astron. Astrophys. **297** (1995) 83 .

[11] S. Philipp et al., Astron. Astrophys. **348** (1999) 768 .

[12] F. Aharonian *et al.* [The HESS Collaboration], Astron. Astrophys. **425** (2004) L13 [arXiv:astro-ph/0408145].

[13] The AUGER collaboration, *The Pierre Auger Observatory Design Report*, 2nd edition, 1997 (http://www.auger.org).

[14] N. Hayashida *et al.* [AGASA Collaboration], Astropart. Phys. **10** (1999) 303 [arXiv:astro-ph/9807045].

[15] W. Bednarek, Mon. Not. Roy. Astron. Soc. **331** (2002) 483 [arXiv:astro-ph/0112008].

[16] L. A. Anchordoqui, H. Goldberg, F. Halzen and T. J. Weiler, Phys. Lett. B **593** (2004) 42 [arXiv:astro-ph/0311002].

[17] J. A. Bellido, R. W. Clay, B. R. Dawson and M. Johnston-Hollitt, Astropart. Phys. **15** (2001) 167 [arXiv:astro-ph/0009039].

[18] M.J. Reid, Ann. Rev. Astron. Astrophys. **31** (1993) 345.

[19] J. A. Davidson et al., Astrophys. J. **387** (1992) 189.

[20] M. A. Gordon, U.Berkermann, P. G. Mezger, Astron. Astrophys. **280** (1993) 208 .

[21] A. L. Coil, and P. T Ho, Astrophys. J. **533** (2000) 245.

[22] M. G. Wolfire, A .G. Tielens, D. Hollenbach, Astrophys. J. **358** (1990) 116.

[23] G. Novak et al., Astrophys. J. **529** (2000) 241.

[24] H.A. Mayer-Hasselwander et al., Astron. Astrophys. **335** (1998) 161.

[25] K. Kosack *et al.* [The VERITAS Collaboration], Astrophys. J. **608** (2004) L97 [arXiv:astro-ph/0403422].

[26] K. Tsuchiya *et al.* [CANGAROO-II Collaboration], Astrophys. J. **606** (2004) L115 [arXiv:astro-ph/0403592].

[27] M. Fatuzzo and F. Melia, Astrophys. J. **596** (2003) 1035 [arXiv:astro-ph/0302607].

[28] P. Blasi and S. Colafrancesco, Astropart. Phys. **122** (1999) 169 [arXiv:astro-ph/9905122].

[29] V. S. Berezinsky, P. Blasi and V. S. Ptuskin, Astrophys. J. **529** (1997) 529 [arXiv:astro-ph/9609048].

[30] G. R. Blumenthal, Phys. Rev. D **1** (1970) 1596.

[31] M. J. Chodorowski, A. D. Zdziarski and M. Sikora, Astrophys. J. **400** (1992) 181.

[32] J. L. Puget, F. W. Stecker and J. H. Bredekamp, Astrophys. J. **205** (1976) 638.

[33] F. W. Stecker and M. H. Salamon, Astrophys. J. **512** (1992) 521 [arXiv:astro-ph/9808110].

[34] S. Eidelman *et al.* [Particle Data Group], Phys. Lett. **B592** (2004) 1.

[35] P. L. Ghia [Auger Collaboration], Proceedings of the 28th International Cosmic Ray Conference (ICRC 2003), Tsukuba, Japan, arXiv:astro-ph/0308428.

[36] G. A. Medina Tanco and A. A. Watson, Proceedings of the 27th International Cosmic Ray Conference (ICRC 2001), Hamburg, Germany, 2001.

[37] M. Bossa, S. Mollerach and E. Roulet, J. Phys. G **29** (2003) 1409 [arXiv:astro-ph/0304023].

[38] M. Nagano and A. A. Watson, Rev. Mod. Phys. **72** (2000) 689.

[39] F. Aharonian and A. Neronov, arXiv:astro-ph/0503354.

[40] T. Sjostrand, L. Lonnblad, S. Mrenna and P. Skands, "PYTHIA 6.3: Physics and manual," arXiv:hep-ph/0308153.

[41] L. O. Drury, F. A. Aharonian and H. J. Voelk, Astron. Astrophys. **287** (1994) 959.